JOURNAL OF CATALYSIS 64, 51–67 (1980)

Activity Measurements and ESCA Investigations of a V_2O_5/SnO_2 Catalyst for the Vapor-Phase Oxidation of Alkylpyridines

S. LARS T. ANDERSSON AND SVEN JÄRÅS

Department of Chemical Technology, The Lund Institute of Technology, Chemical Center, Box 740, S-220 07 Lund 7, Sweden

Received July 19, 1978; revised November 30, 1979

Calibration curves for the quantitative ESCA analysis of a V_2O_5/SnO_2 catalyst have been constructed. It is shown that by sintering the catalyst the SnO_2 particles are embedded in a V_2O_5 matrix, and that the surface concentration of V_2O_5 is higher than the stoichiometric bulk composition. Product distributions for the oxidation of 3-picoline and 2-methyl-5-ethylpyridine (MEP) over the catalyst V_2O_5/SnO_2 = 1/1.5 are reported. Activation of the catalyst during the first 30–60 min can be correlated with its degree of reduction, which is increasing during this period. The catalyst is only reduced in a thin surface layer to an oxidation state somewhere between V_2O_5 and V_2O_4. Simultaneously the amount of adsorbed species, which are suggested to be adsorbed intermediates, is increasing. A decrease in the ratio O_2/3-picoline produces an increased total oxidation in the conversion over the V_2O_5/SnO_2 catalyst 1/1.5. The degree of reduction of the catalyst as well as the amount of adsorbed species is simultaneously increased. The addition of H_2O to the vapor phase increases both the conversion and the selectivity. The catalyst is less reduced with the addition of H_2O. The pyridine derivatives are shown to be adsorbed on the catalyst without any large donation of the electron pair of the N atom. Adsorption via the alkyl carbon of an oxidized intermediate is suggested. A shift of 1.7 eV in the N_{1s} core line indicates that of the pyridine carboxylic acids in the solid state only picolinic acid forms hydrogen bonds to the N atom. The equilibrium distribution between H-bonded and non-H-bonded picolinic acid is 2 : 3.

INTRODUCTION

For the manufacture of 2-pyridinecarboxylic acid (picolinic acid) and 3-pyridinecarboxylic acid (niacin) on an industrial scale liquid-phase oxidation is employed. 2-Picoline is oxidized by potassium permanganate to picolinic acid and a convenient 3-alkylpyridine, i.e., 3-picoline or 2-methyl-5-ethylpyridine (MEP) is oxidized with nitric acid and high pressure. However, if air could be used as the oxidizing agent without significantly reducing the yields, the cost would be lowered and the production simplified.

The oxidation of 2-picoline to picolinic acid and 2-pyridinealdehyde in the vapor phase using air as the oxidizing agent has already been studied (*1*) and 3-picoline (*2*) and MEP (*3*) have been used similarly. In these experiments, catalysts based on V_2O_5 have chiefly been used. Generally it has been observed that during the course of oxidation the catalyst becomes reduced (*4*), and the catalytic mechanism is often described as a redox process (*5*). However, as a rule the whole bulk phase of the catalyst has been analyzed. The aim of the present investigation was to study how the surface layer of a V_2O_5-based catalyst is affected by participating in the catalytic oxidation of 2-picoline, 3-picoline, and MEP.

Recently, ESCA (electron spectroscopy for chemical analysis) has been increasingly used for investigating catalysts (*6*). It is a surface-sensitive analytical method that gives information about elements present in a surface layer of approximately 10–50 Å. Their oxidation states and/or chemical environment can usually also be determined. Quantitative analysis (*7*) is becoming more common, in spite of the fact that the error can be as large as 50%. However, the factors causing any inaccuracy in the

0021-9517/80/070051-17$02.00/0

present work are stated and methods for minimizing them are discussed. Due to the samples being rather similar to each other, and by using careful calibration the error has been lowered to well under 10%. The states of vanadium, tin, and especially oxygen in catalyst $V_2O_5/SnO_2 = 1/1.5$ treated in various ways are analyzed both qualitatively and quantitatively and are discussed below.

It was already known that the catalyst is reduced, and V_6O_{13} particularly has been described as being a selective oxidant (*8, 9*), while V_2O_5 and V_2O_4 alternately are described as being inactive or active for total oxidation, depending upon which substances are being oxidized. It was therefore of interest to look for correlations between the product distribution and surface state of the catalyst for the reactants here employed.

An activation phenomenon can often be observed in catalysis, and for V_2O_5 catalysts it has been described as a reduction of the catalyst (*8*). This modification during the oxidation of 2-picoline and MEP was studied for a period of 2.5 h. Since other parameters and additions that can influence the conversion may also affect the catalyst, we also investigated how the ratios O_2/3-picoline and O_2/MEP influence the conversion to the various main products and the surface state of the catalyst, and how the addition of H_2O affects the catalyst.

To gain insight into the reaction mechanism, it is necessary to know both the state of the catalyst and how the reactants are adsorbed on the catalyst. There is little information on how pyridine derivatives are bonded to the surface, but a shift in the N_{1s} binding energy using ESCA should show whether or not they are coordinated by the N lone pair.

METHODS

Instrumental

The experiments were performed on an AEI ES 100 electron spectrometer equipped with a hemispherical electrostatic analyzer. An Al anode (1486.6 eV) was used, and the instrumental resolution for the $Au_{4f_{7/2}}$ signal was 1.3 eV. The oil diffusion pumps gave a vacuum of 10^{-7}–10^{-8} Torr. The instrument was calibrated as described earlier by Schön (*10*). To adjust the signals for the sample charging, which was smaller than 1 eV for these samples, the C_{1s} signal from the carbon compound in the sample was observed and was given the binding energy (BE) value of 284.3 eV, which is the position of carbon in graphite (*11*). If the samples were kept in the spectrometer for a long period of time a carbon signal at 285.0 eV built up; this originated from the pump oil (*11*) which was slowly contaminating the sample surface. This of course makes the charging adjustment difficult. The carbon signal from the series with different reaction times was often unsymmetrical and the right-hand O_{1s} signal (at lower BE) was used for calibration and placed at 529.7 eV instead.

X-Ray diffraction analysis was carried out by a Philips X-ray diffraction instrument using a PW 1310/01/01 generator and CuKα radiation.

Secondary ion mass spectroscopy (SIMS) was performed on a Cameca IMS 300 instrument. The probe size was $\approx$200 μm. The primary ion (O^-) current was $=0.4$ μA. Secondary ions were positive.

Sample preparation

V_2O_5 was from UCB (PA) and Baker (AR). Sn and SnO were from Kebo (purum), SnO_2 was from Fisher (certified reagent grade). $Sn(VO_3)_4$ was precipitated from a solution of $SnCl_4$ (BDH, laboratory reagent grade) with NH_4VO_3 (Riedel de Haen, purum), washed and dried at 100°C. The following pyridine derivatives were used: picolinic acid (2-pyridinecarboxylic acid, Merck P.A.), nicotinic acid or niacin (3-pyridinecarboxylic acid, Merck P.A.), isonicotinic acid (4-pyridinecarboxylic acid, Merck P.A.), isocinchomeronic acid (2,5-pyridinedicarboxylic acid, Fluka AG

lab use), 3-pyridinecarbaldehyde (Merck P.A.), niacin N-oxide (AB Bofors, Nobelkrut), isonicotinic acid N-oxide (AB Bofors, Nobelkrut), 3-picoline (3-methylpyridine, Merck P.A.), and pyridine (Mallinckrodt AR).

The catalysts were made by sintering V_2O_5/SnO_2 powder mixtures (ratio 1/1.5) at 1250°C for 3 h. Calibration curves for the ESCA analysis were constructed both for the V_2O_5/SnO_2 powder mixtures ground in a Retsch mill and the same samples sintered in quartz crucibles at 1250°C and thereafter ground in the mill.

For the ESCA measurements, the catalyst granules were placed, or the powder pressed, into a boat sample holder. No contribution from the sample holder could be seen in the spectra.

The catalysts were analyzed within a few hours after their use in catalytic oxidation. The transfer from the catalytic reactor to the ESCA instrument was done in air. No changes could be detected in catalysts stored in air for 2 weeks, as compared with samples transferred in nitrogen.

The catalysts that had been used for 150 min were also analyzed, after having been ground, to see if the changes had only occurred in the surface layer. These samples were ground manually in an agate mortar. Adsorption measurements were done by slurrying the catalyst with the liquid, inserting the sample into the vacuum of the sample chamber, and quickly cooling the sample probe with liquid nitrogen. The sample was thereafter heated in steps, under vacuum, while spectra were recorded at intervals.

Oxidation Experiments

The catalysts were used as solid-phase catalysts in the vapor-phase oxidation of alkylpyridines. The experiments were performed in an apparatus that included four main units: a feeding system for introducing controlled amounts of alkylpyridine, air, and steam; the catalytic reactor; a product recovery unit; and an analysis unit including a total oxidation reactor.

Primary air was passed through the thermostated vaporizer containing alkylpyridine. The resultant gas stream was mixed with secondary air and steam to the desired composition. The percentage of alkylpyridine in the reactant stream was determined by oxidizing the alkylpyridine totally to carbon dioxide, water, and nitrogen oxides and analyzing the percentage of carbon dioxide by gas chromatography.

The condensing system after the reactor consisted first of three U-tubes, then four bubblers containing water, and finally two tubes packed with glass wool. The first U-tube was kept at −20°C and the last two at −50 and −60°C by means of freezing mixtures. The analyses of the products have been described by Järås (*12*).

Quantitative ESCA Analysis

As a measure of the intensity, the area of each signal was taken (*13*). For the O_{1s}–$V_{2p_{3/2}}$ region the baseline was drawn from the higher BE side of the O_{1s} signal to the lower BE side of the $V_{2p_{3/2}}$ signal. The O_{1s} signal was usually unsymmetrical and it was deconvoluted manually into its two components by a mirror reflection of the low BE side. This procedure is not inferior to a computer treatment.

The areas, measured using a planimeter, were multiplied by the counting rate and divided by the sensitivity factor for photoemission. Atom percentages of V, Sn, and O were calculated by dividing each figure by the sum (Σ) of all three. C/Σ and O_{ad}/Σ were also calculated.

The sensitivity factors for photoemission used here were $C_{1s} = 0.37$, $N_{1s} = 0.63$, $O_{1s} = 1$, $V_{2p_{3/2}} = 2.17$, and $Sn_{3d_{5/2}} = 7.0$. They were determined by measurements on the clean oxides. The arithmetic mean values of sintered and unsintered samples were calculated. C_{1s} and N_{1s} sensitivity factors were taken from Carter *et al.* (*14*) and were adjusted to the base $O_{1s} = 1$.

All lines in the figures are least-squares fits performed on an HP 9100B desk calculator with a 9125A plotter. The curve deconvolution of the N_{1s} core line of picolinic acid was performed on the same equipment using Gaussian curve forms.

RESULTS AND DISCUSSION

Quantitative ESCA Analysis

In measuring element concentrations by ESCA, several factors of importance must be taken into account (*15, 16*). These are both pure instrumental and sample factors. As these experiments have been performed on a single instrument and with the same conditions for different samples (intensity of the X rays, sample orientation, collector and analyzer widths), the instrumental factor has been minimized. The other factors can be reduced by measuring samples as much alike as possible and keeping the same orientation of the samples in the spectrometer. By also choosing closely lying signals ($O_{1s} \rightarrow V_{2p_{3/2}} - Sn_{3d_{5/2}} = 954 - 967 - 998$ eV) for the various elements, the variation in losses, due to inelastic scattering, can be ignored.

The intensity then depends upon the number of atoms in the volume element and the probability for emission, which varies with element and core. The cross sections for photoemission can be found in the literature both experimentally determined (*17*) and theoretically calculated (*14, 16*). The cross sections can vary by a considerable amount for the same element in different compounds (*18*). Attempts to explain this have been made (*13, 16, 18*), but it is still not possible to foresee these variations, and therefore calibrations have been performed here.

In Fig. 1, curves of atom percentage V and Sn, determined by the ESCA analysis, are shown as a function of the theoretical composition of the samples. The reproducibility of the ESCA analysis is measured for the catalyst sample to be less than the following values: 2% error in the area measurement, 5% error in the recording of the spectra, 5% error in the preparation of the sample. The mean square of these errors is

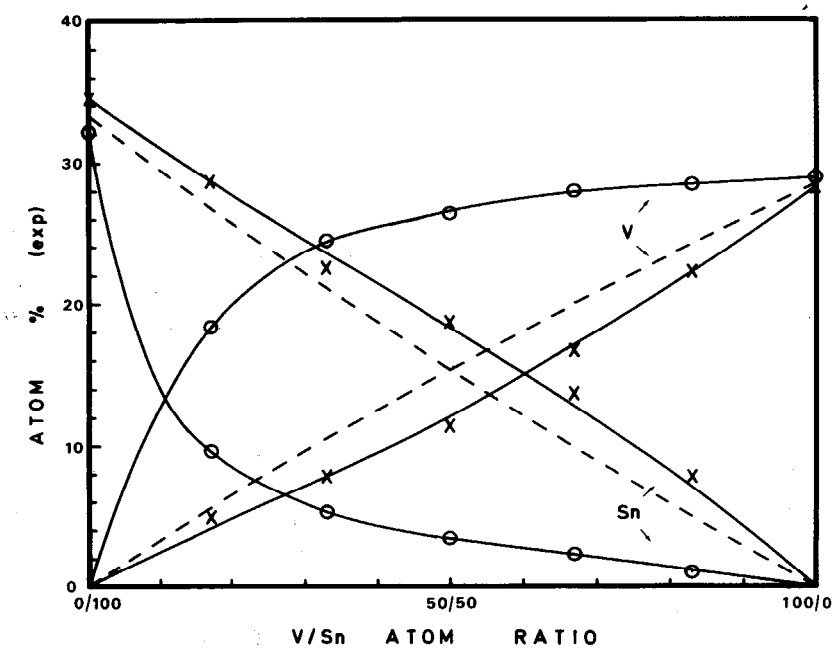

FIG. 1. Composition in atom percentage V, Sn, and O calculated from ESCA spectra of V_2O_5 and SnO_2 mixtures as a function of the V/Sn bulk ratio for both sintered (O) and unsintered (X) samples.

less than 8%. In Table 1 the composition in atom percentage for the various oxides is shown. The deviation from the theoretical values is rather low.

In Fig. 1, one can see that for powder mixtures the curve for percentage Sn is somewhat higher than the theoretical curve (dashed line) and for percentage V is somewhat lower. If the SnO_2 particles are smaller than the V_2O_5 particles, SnO_2 will occupy a relatively larger portion of the surface than the true composition in the bulk would indicate, due to a pure packing effect. The same effect has been observed in the systems V_2O_5–SiO_2 and V_2O_5–TiO_2. Similar results are reported for MoO_3–SnO_2 (*19*). It has also been observed that the deviation is larger if the particle sizes of the oxides are very different. For powder mixtures that had not been ground in a Retsch mill, but yet mixed very thoroughly with a spatula, the effects were very large.

For the sintered mixtures, a much larger deviation in percentage V and percentage Sn from the theoretical values is apparent.

TABLE 1

The Composition of Some V and Sn Oxides and the V_2O_5/SnO_2 Catalyst (1/1.5) Before and After Reaction, with or without Water Addition[a]

	Composition (atom%)			C/Σ	O_{ad}/Σ
	O	V	Sn		
SnO	56		44		0.18
SnO, theory	50		50		
SnO_2	65.5		34.5		0.06
SnO_2, sintered	67.9		32.1		0.07
SnO_2, theory	66.7		33.3		
$Sn(VO_3)_4$	70.8	21.5	7.7		—
$Sn(VO_3)_4$, theory	70.6	23.5	5.9		
V_2O_5	71.8	28.2			0.19
V_2O_5, sintered	71.1	28.9			0.16
V_2O_5, theory	71.4	28.6			
V_2O_5/SnO_2 (1/1.5), theory	69.6	17.4	13.0		
V_2O_5/SnO_2, used (MEP) (with water)	70.0	25.2	4.8	0.62	0.22
V_2O_5/SnO_2, used (MEP) (without water)	68.5	25.4	6.2	0.66	0.33
V_2O_5/SnO_2 unused[b]	70	27	3		

[a] Compositions are given in atom% V, Sn, and O and for C and O_{ad} as the ratio to the sum of V + Sn + O.

[b] Taken from curves of sintered V_2O_5/SnO_2 mixtures in Fig. 1.

The curves intersect each other at a theoretical V/Sn ratio of approximately 10/90 and analysis gives 14% V and 14% Sn. The cause of this is that the sintering is done at 1250°C, a temperature between the melting point of both components. The melting point of V_2O_5 is 690°C while that of SnO_2 is approximately 1600°C, and it seems likely that the SnO_2 particles will be surrounded by V_2O_5 on cooling. The presence of the separate V_2O_5 and SnO_2 phases was identified with X-ray diffraction and scanning secondary ion mass spectroscopy. The distribution of Sn is shown in Fig. 2. From this analysis it is clear that SnO_2 exists mostly as separate aggregates in the V_2O_5 phase. Any conclusions regarding doping effects in this system cannot be drawn from these investigations, but such effects seem plausible.

In Table 1 it is shown, by the ESCA analysis, that the used catalyst V_2O_5/SnO_2 = 1/1.5 has an Sn content of approximately 5%. This is a rather large deviation from the theoretical, 13.04% Sn. However, from Fig. 1, at the theoretical composition of this catalyst (V/Sn = 57.14/42.86), it can be seen that this sample in powder mixture gives 17% Sn while the sintered mixture only gives 3% Sn in the ESCA analysis.

The O_{1s} signal was asymmetric for all of the measured samples. It can be seen from Fig. 6 that this asymmetry toward higher BE is greater for the used catalysts. The origin of the asymmetry is thought to be that oxygen is adsorbed in various forms on the surface of these oxides, and thus gives a signal at a higher binding energy than lattice oxygen. Asymmetry due to core hole–conduction electron interaction is considered to be negligible since the density of states is low. The contribution that gives the asymmetry in the O_{1s} line has been separated from the main line. It is termed O_{ad} and has approximately 2 eV higher binding energy. The main signal has been calculated as percentage O and the other signal as the ratio to the sum of O, V, and Sn, i.e., O_{ad}/Σ.

FIG. 2. Photograph from scanning SIMS (mass number 120) showing an inner part (polished) of catalyst with V_2O_5/SnO_2 = 1/1.5. The diameter of the area is 100 μm. The large black part is probably a nick. The white parts correspond to Sn. Sn is available mainly as small grains (2–6 μm). Where Sn is available dark shadows are seen on the V picture.

Other possible contributions to asymmetry have been excluded because broadening to higher BE occurs only for the O_{1s} signal. This asymmetric oxygen signal from metal oxides has been explained as adsorbed OH groups and O_{ad}^- (*20*) or quite generally as one or several oxygen forms of the type OH^-, H_2O, O_2, CO_3^{2-} (*21*). All of these species should have a higher binding energy than O_2^- in the lattice and give a contribution to the part of the O_{1s} signal that here has been separated from the main signal.

The Product Distribution and Reaction Scheme for the Oxidation of Pyridine Derivatives with the Catalyst V_2O_5/SnO_2 = 1/1.5

The variation of the temperature for the oxidation of 3-picoline and MEP with catalyst V_2O_5/SnO_2 = 1/1.5 gave a product distribution according to Fig. 3, which shows the conversion to the different oxidation products per mole of the alkylpyridine in the feed.

In the oxidation of 3-picoline by air over this catalyst, the percentage of pyridine was consistently low. The amount of carbon oxides formed by total oxidation increased continuously with increasing temperature.

In the case of 2-picoline a similar product distribution was obtained, but differed considerably at one point. The picolinic acid formed was rapidly decarboxylated and only 2–3% acid was obtained. Instead 2-pyridinealdehyde was formed in rather large amounts at the lower temperatures and pyridine at somewhat higher temperatures, before the total oxidation started at the highest temperatures.

In the oxidation of MEP a "tar product," which among other things probably contained polymerization products of vinylpyridines, was obtained. Isocinchomeronic

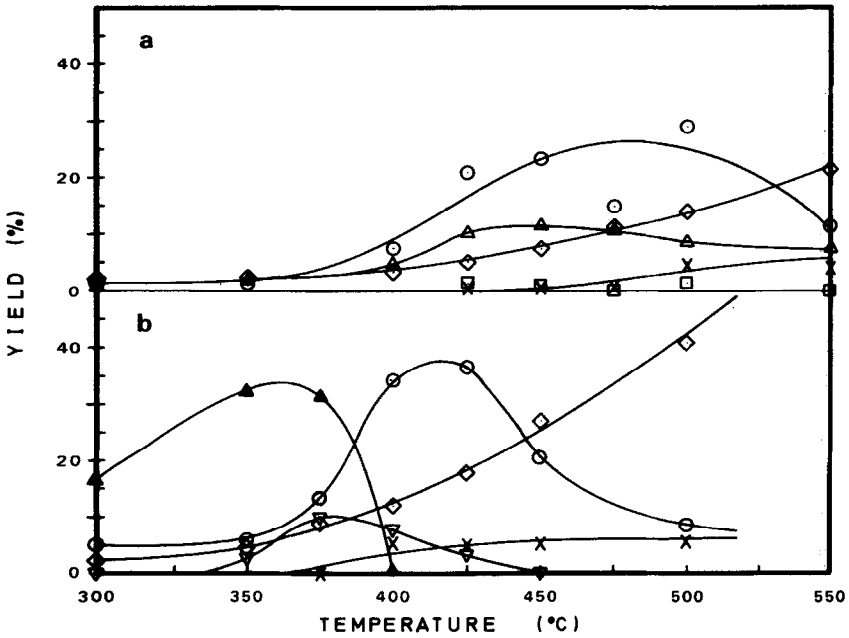

FIG. 3. The conversion (mole%) to various products over catalyst V_2O_5/SnO_2(= 1/1.5) calculated per mole of incoming 3-picoline (a) or MEP (b) as a function of temperature.

	(a)	(b)
Mole ratio		
O_2/alkylpyridine	41	53
H_2O/alkylpyridine	88	109
Space velocity (h^{-1})	6000	3700

(○) Niacin, (△) 3-pyridinealdehyde, (▲) 5-ethyl-2-pyridinealdehyde, (▽) 5-ethylpyridine, (◇) carbon dioxide, (□) carbon monoxide, (X) Hydrogen cyanide. The catalysts have been activated for 60 min at each temperature in order to obtain a steady state.

acid, which is obtained as an intermediate in the liquid-phase oxidation of MEP, is not obtained at all as a product in the vapor-phase oxidation.

The percentage of 2-methyl-5-vinylpyridine is generally below 1% and 3-vinylpyridine somewhat higher. The percentage of 3-pyridinealdehyde is low, either because it is rapidly oxidized to niacin or it is not an important intermediate for niacin. Furthermore, the percentage of pyridine does not normally exceed 3% at any temperature. The thermal decarboxylation of niacin is only a few percent under these conditions.

At higher temperatures, small amounts of maleic acid, formed by the destruction of the pyridine ring, are found. The total oxidation products, carbon dioxide, carbon monoxide, and hydrogen cyanide, like the tar products, increase in yield with increasing temperature.

The Effect of Reaction Time on the Catalyst V_2O_5/SnO_2 = 1/1.5

In the catalytic vapor-phase oxidation with vanadium pentoxide catalyst in a fixed bed (*4*) there is usually a variation of the oxidation state in the bed. In order to obtain an even oxidation state throughout the bed, the experiments were performed in the following way: the melted and resolidified catalyst (V_2O_5/SnO_2 = 1/1.5)

was crushed and sifted to obtain a fraction <80 mesh, and the catalytic reaction was carried out in a fluidized bed. Small samples of the catalyst were withdrawn from the bed every 15 min by immersing a small bowl in the bed.

The conversion of 2-picoline (mole%) to 2-pyridinealdehyde and carbon dioxide per mole of incoming 2-picoline as a function of the catalyst lifetime in the reactor is shown in Fig. 4. These values were obtained by condensing the products during 30 min and they are thus the average value for this period. The formation of carbon dioxide in the oxidation of MEP over the same catalyst as above is also shown, in milligrams per minute.

The latter were obtained by adsorption of CO_2 in ascarite–dehydrite during periods of from 5 to 30 min and are thus the average values during these periods. In these two last series of experiments, the catalyst bed was not fluidized during the experiments. As seen from Fig. 4, a stationary state was obtained after 30–60 min; the same product distribution was obtained for up to 6.5 h thereafter.

The results of the ESCA analysis of the catalysts used in the 2-picoline oxidation above are shown in Figs. 4, 5, and 6. First, one should notice the difference between the theoretically and experimentally determined compositions already mentioned. The analysis of the 150-min sample after grinding is also shown. The surfaces of the catalyst granules have disappeared in the new surfaces of fracture that are uncovered and the ground sample is completely identical to unused catalyst.

In Table 2 O_{1s}, $Sn_{3d_{5/2}}$, and $V_{2p_{3/2}}$ binding

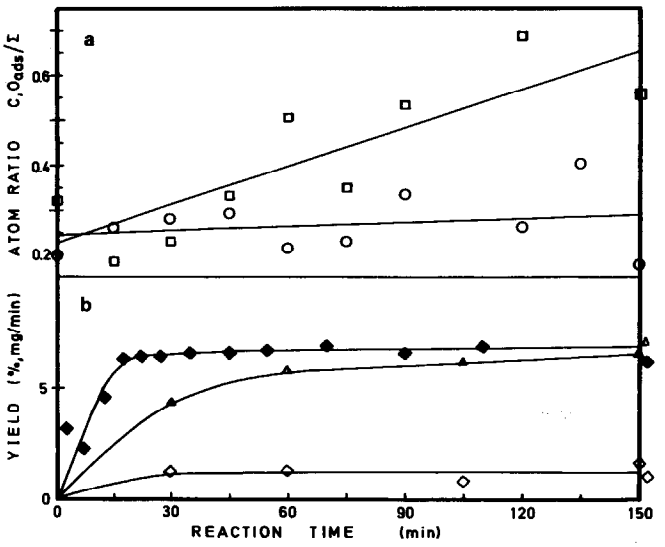

FIG. 4. (a) The atom ratios C/Σ and O_{ad}/Σ calculated from ESCA spectra for the catalyst V_2O_5/SnO_2 (=1/1.5) used for various reaction times in the oxidation of 2-picoline. (□) C/Σ and (○) O_{ad}/Σ, where Σ = V + Sn + O. (b) The conversion of 2-picoline (mole%) to 2-pyridinealdehyde (△) and CO_2 (◇) and of MEP (mg/min) to CO_2 (◆) in the oxidation over V_2O_5/SnO_2 (=1/1.5). Signs at the right side of the right axis indicate mean values from 150 to 360 min.

	2-Picoline	MEP
Mole ratio		
O_2/alkylpyridine	12	75
H_2O/alkylpyridine	—	175
Temperature (°C)	375	450

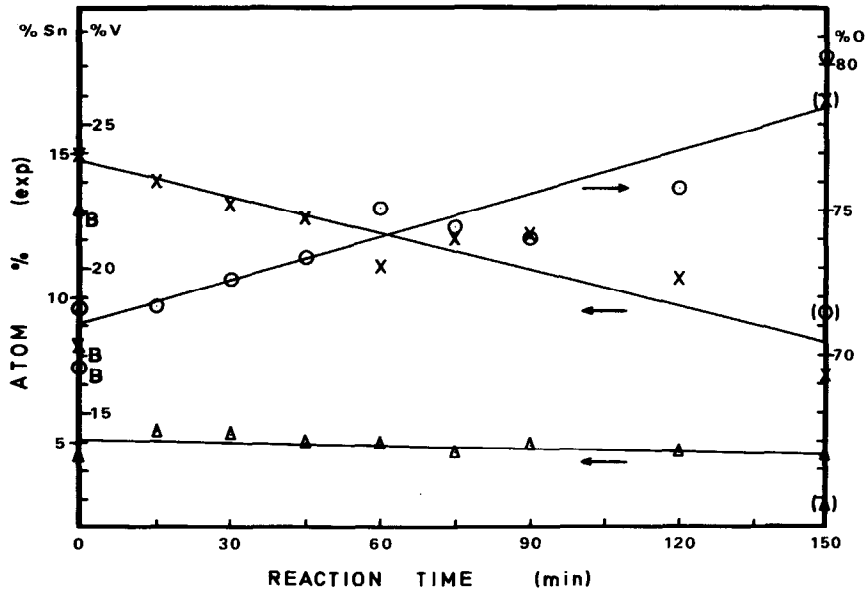

FIG. 5. The composition in atom percentage V (X), Sn (Δ), and O (O) calculated from ESCA spectra for the catalyst V_2O_5/SnO_2 = 1/1.5 as a function of the reaction time for the oxidation of 2-picoline. Points marked "B" are stoichiometric bulk compositions, while those within parentheses are for ground 150-min samples.

energies for the various samples are shown. These have been adjusted using the dominant O_{1s} peak at lower BE, i.e., lattice oxygen which is considered to have a fairly constant value, 529.7 eV. There was a clear change in the spectral features for catalysts used for 15 min, or more, as compared with unused catalyst (0 min). All signals were broadened, but without any large change in binding energy. As the charging was very small the possibility of a differential charging causing the increase in FWHM (full width at half-maximum) can be eliminated and it must be concluded that SnO_2 and V_2O_5 have been reduced partially in the surface layer. Unused catalyst (0 min) consists of V_2O_5 and SnO_2 only (Table 2). It seems reasonable to assume tha SnO_2 in the used catalyst has been partially reduced to SnO, considering the broadened $Sn_{3d_{5/2}}$ line. This is in accordance with ESR (*28*) and uv (*29*) measurements, which have shown that SnO_2 is reduced by propene and butene yielding both Sn^{3+} and Sn^{2+} in the surface layer.

When explaining the broadening of the O_{1s} and $V_{2p_{3/2}}$ signals it is useful to look at the curve shapes in Fig. 6. The first curve is the sample at 0 min and the next two are at 15 and 120 min, respectively. The difference in curve shape between these samples is that the O_{1s} signal is broadened unsymmetrically toward higher BE and the $V_{2p_{3/2}}$ signal toward lower BE as the reaction time increases. This can be explained by an increase in the amount of adsorbed oxygen and by V_2O_5 being partially reduced to V^{4+} and perhaps also to a lower valence state. Shulga *et al.* (*30*) and Valdelièvre *et al.* (*31*) also found a broadening of the $V_{2p_{3/2}}$ signal caused by the reduction of the catalyst during catalysis. It should be mentioned that even pure V_2O_5 is a nonstoichiometric oxide with oxygen vacancies that are compensated by V^{4+} and possibly V^{3+} (*32*). However, it can be seen from the spectra of the sample at 0 min that this amount is below the detection limit. The sample at 150 min after grinding shows the same spectral features as the sample at 0 min, in

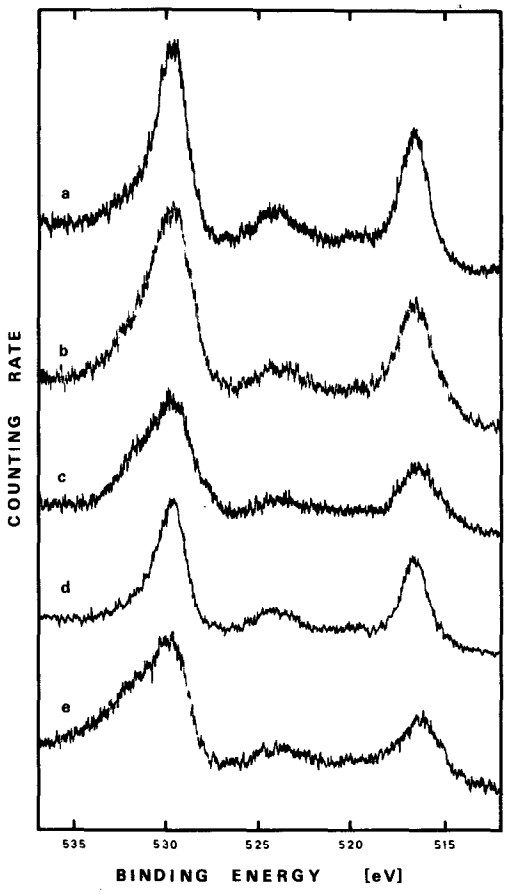

FIG. 6. O_{1s} and V_{2p} electron spectra from the catalyst V_2O_5/SnO_2 = 1/1.5 used for various reaction times in the oxidation of 2-picoline. (a) 0 min, (b) 15 min, (c) 120 min, (d) 150-min. ground, and (e) unused catalyst, after wetting with 3-pyridinecarbaldehyde at −50°C, followed by heating to 350°C and evacuation for spectroscopic measurement.

accord with the surface layer only being altered. This suggests that an equilibrium is being established and that the amount of reduction is determined by the reducing capability of the reactant phase and the kinetics. It is not possible to say which phase is active, but it is clear that the catalyst is reduced to a state between V_2O_5 and V_2O_4 in a rather thin surface layer. It may be that the activation time, as described in the activity measurements, is associated with the formation of an active phase that is probably V_6O_{13}.

Considering the results of the quantitative analysis shown in Fig. 5, larger and more continuous effects are observed. The atom percentage V and Sn diminish with increasing reaction time and the percentage O increases with reaction time. The apparent change in the V/Sn ratio may be caused by a reorganization in the surface layer. It was shown above that the catalyst was partly reduced during use. This implies that the percentage O is diminishing and the percentage V is increasing in contradiction to the quantitative results. An explanation for this might be that a part of the lower BE O_{1s} signal consists of adsorbed oxygen in some form, and that this part is increasing with reaction time.

The amounts of adsorbed oxygen and carbon species (O_{ad}/Σ and C/Σ) were observed to increase with reaction time (see Fig. 4). It is possible to compare the increase in O_{ad}/Σ and C/Σ during the reaction to obtain some idea of what species it may be. From 0 to 150 min, the increases were 0.06 for O_{ad}/Σ and 0.42 for C/Σ. From the intensity of the N_{1s} line for the sample at 150 min, an N/Σ ratio of 0.065 is calculated. Thus, an N:O: ratio of approx 1:1:7 is obtained, which should represent the elemental ratio of the adsorbed species. It is not possible to make any definite statements concerning what species may be present on the surface. However, it seems reasonable that this species is either a product or an intermediate. Plausible adsorbed species containing oxygen that can exist during the catalytic reaction are OH^-, O_2 (various forms), CO, CO_2, H_2O, Py-COOH, and Py-CHO. There may of course also be some species which do not contain oxygen. O_{ad} has about 2 eV higher binding energy than lattice oxygen (see Table 2), but it is not possible to assign a specific form. VOH has been identified by ion microanalysis, and these groups are of course contributing to the O_{ad} signal, but not in any detectable amount because of the low concentration (0.5–1%). From a comparison with literature data from ESCA studies of adsorption

TABLE 2

O_{1s}, $V_{2p_{3/2}}$, and $Sn_{3d_{5/2}}$ Electron Binding Energies and Half-Widths (eV) for Some V and Sn oxides and the V_2O_5/SnO_2 Catalyst Used for Various Periods (0–2.5 h) in the Vapor-Phase Oxidation of 2-Picoline

	$O_{(ad)1s}$	O_{1s}	$Sn_{3d_{5/2}}$	$V_{2p_{3/2}}$	Ref.
V_2O_5[a]	531.5	529.6 (1.6)		516.6 (1.5)	
SnO_2[a]	531.4	529.7 (1.6)	486.1 (1.8)		
SnO[b]	532.0	529.8 (2.4)	485.9 (2.5)		
Sn	531.5	529.8 (2.0)	485.7 (2.0)–484.1 (1.8)		
$Sn(VO_3)_4$	531.6	529.6 (1.8)	486.2 (1.6)	516.6 (1.5)	
V	531.7	530.3		512.4 (1.2)	*22*
V_2O_5	530.9	529.6		516.6 (1.5)	*22*
V				512.7 (2.0)	*23*
VO_2		529.6 (2.4)		515.7 (3.2)	*23*
V_2O_5		529.9 (2.0)		516.8 (1.7)	*23*
V_2O_5				517.6	*24*
VO_2				517.6 + 516.5	*24*
V_2O_3				517.6 + 516.5 + 515.6	*24*
Sn			486.4–485.2		*25*
SnO_2			487.2		*25*
SnO			485.9		*26*
SnO_2			486.0		*26*
Sn			484.1		*27*
SnO		529.9	485.8		*27*
SnO_2		530.3	486.3		*27*
V_2O_5/SnO_2 Catalyst					
0 min	531.8	529.7 (1.8)	486.0 (1.8)	516.6 (1.7)	
15–150 min,[c]	532.1	529.7 (2.5)	485.7 (2.4)	516.5 (2.4)	
150 mg, ground	531.5	529.7 (1.6)	485.8 (1.7)	516.6 (1.7)	

[a] The same results were obtained for V_2O_5–SnO_2 powder mixtures, sintered and unsintered.
[b] Differential sample charging is thought to broaden these lines.
[c] Mean values from nine catalysts used for different reaction times.

on metals one can expect to find the O_{1s} signal from O_2, CO, CO_2, and H_2O in the signal at higher BE and a greater amount of CO and CO_2 in the lower BE part (*33*). In the present work, O_{1s} has been measured for Py-CHO at 532.0 and for Py-COOH at 531.4 eV (see Table 3).

The O_{1s} and V_{2p} spectra from adsorbed pyridinecarbaldehyde on catalyst V_2O_5/SnO_2 = 1/1.5 in vacuum at 350°C is shown at the bottom of Fig. 6. The similarity between this spectrum and that from the catalyst used for 120 min is clearly seen. It is possible that the observed increase in O_{ad}/Σ and C/Σ is caused by an adsorption of some intermediate, e.g., pyridinecarbaldehyde, increasing with reaction time. This is supported by the C_{1s} signal having a binding energy of approx 284.7–284.9 eV, typical of a hydrocarbon. The stoichiometry N : O : C = 1 : 1 : 6 for the adsorbed carbaldehyde is of the same magnitude as the species observed after catalysis. However, it is not known if only one species is adsorbed, and the ratio N : O : C = 1 : 1 : 7 could be composed of an intermediate, as well as adsorbed oxygen in some form and carbon contamination.

Dependence of the Reaction upon the Amount of 3-Picoline on Catalyst V_2O_5/SnO_2 = 1/1.5

In Fig. 7 unconverted 3-picoline and conversions to the various oxidation products are given as a function of the molar ratio O_2/3-picoline for catalyst V_2O_5/SnO_2 =

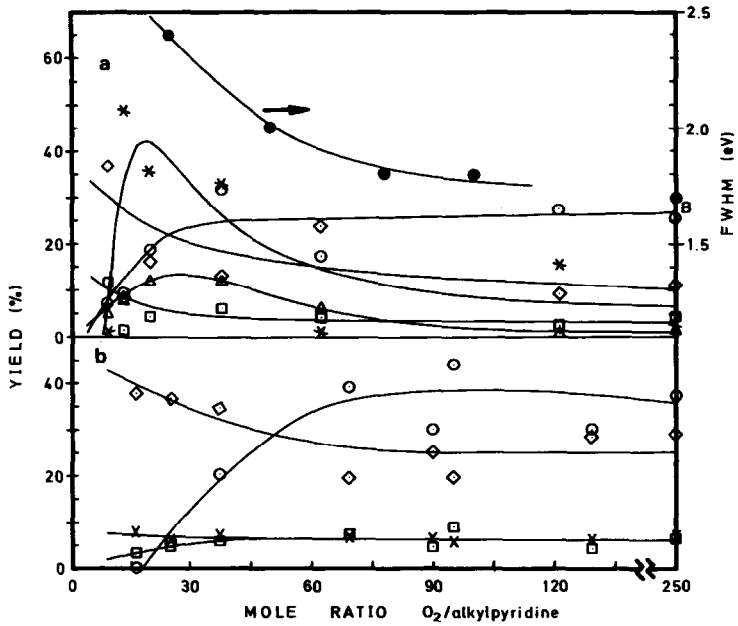

FIG. 7. The conversion to the various products in the oxidation over V_2O_5/SnO_2 (= 1/1.5) calculated per mole of incoming 3-picoline (a) or MEP (b) as a function of the mole ratio O_2/alkylpyridine.

	(a)	(b)
Mole ratio		
O_2/alkylpyridine	8–250	16–250
H_2O/alkylpyridine	98–98	34–406
Space velocity (h^{-1})	4300–1700	3640–3640
Temperature (°C)	450–450	400–400

(*) 3-picoline (unconverted), (○) niacin, (△) 3-pyridinealdehyde, (◇) carbon dioxide, (□) carbon monoxide, (X) hydrogen cyanide. On the right axis are shown FWHM (eV) for the $V_{2p_{3/2}}$ line (●). Value marked "B" is for unused catalyst, representing a large O_2 surplus.

1/1.5. The corresponding values for the oxidation of MEP are also given.

As is shown by the figures the yield of niacin is low at low ratios of O_2/alkylpyridine, while simultaneously the total oxidation to CO and CO_2 is high. At a higher ratio the yield of niacin is higher and simultaneously the total oxidation has diminished.

From the ESCA spectra of these samples no alterations in the O_{1s} or $Sn_{3d_{5/2}}$ binding energies or half-widths could be detected. In contrast, $V_{2p_{3/2}}$ is lowered by 0.3 eV in the binding energy and unsymmetrically broadened from 1.8 to 2.4 eV (see Fig. 7). This indicates that with an increased concentration of 3-picoline the catalyst is reduced more (i.e., V_2O_5), by an undetermined extent.

In Fig. 8 the results of the quantitative ESCA analysis are shown. It appears that atom percentage V and Sn are diminishing with an increase in the concentration of 3-picoline, and that percentage O is increasing. The catalyst is, as seen above, reduced, but still percentage O is increasing and percentage V and Sn are diminishing. This is exactly the same contradictory result as was given above for various reaction times.

One reasonable hypothesis concerning this phenomenon is the following. With

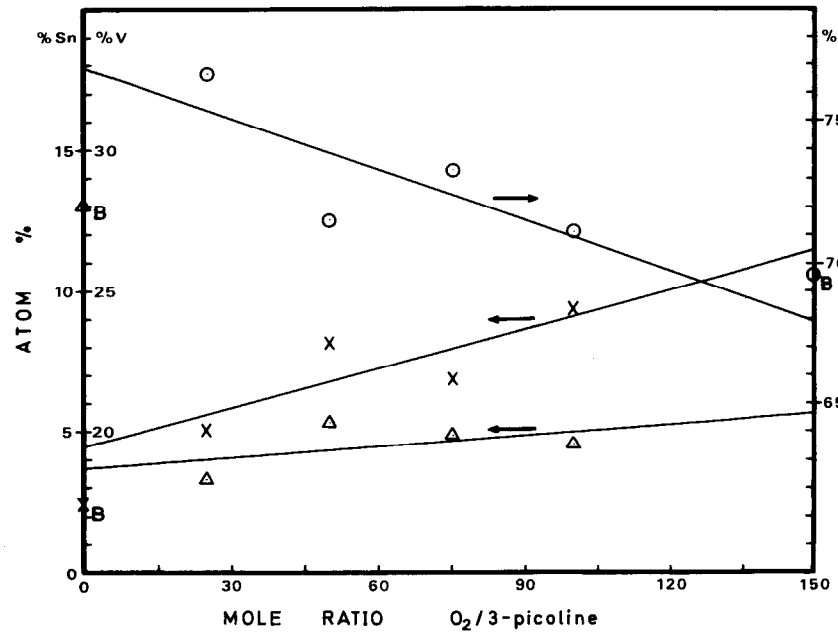

FIG. 8. Composition in atom percentage V (X), Sn (△), and O (○) calculated from ESCA spectra for the catalyst V_2O_5/SnO_2 = 1/1.5 used for the oxidation of 3-picoline, as a function of O_2/3-picoline mole ratio. Values marked "B" are stoichiometric bulk compositions. Operating conditions as in Fig. 7.

increasing concentration of 3-picoline and reaction time for the catalyst the active centers are increasing in concentration, and they are thought to have the ability to adsorb more oxygen than the original catalyst surface.

The Effect of Added H_2O on Catalyst V_2O_5/SnO_2 = 1/1.5 and Its Activity for the Oxidation of Alkylpyridines

In Fig. 9 the formation of niacin and the other products in the oxidation of MEP is given as a function of the molar ratios H_2O/MEP.

By adding steam in a mole ratio H_2O/2-picoline = 82 to the reactants in the oxidation of 2-picoline, the yield of 2-pyridinealdehyde increased from 12 to 44% and the selectivity increased from 33 to 64% at the same time (*34*). Also in the oxidation of MEP (see Fig. 9), the addition of steam has a favorable effect by increasing the conversion and selectivity for the aldehyde and niacin and lowering the extent of partial oxidation.

From the ESCA spectra it was observed that the $V_{2p_{3/2}}$ signal was more asymmetrically broadened toward lower BE (FWHM = 2.5 eV) for catalysts used without steam addition than catalysts used with steam addition (FWHM = 2.0 eV). It is possible that there is correlation between selectivity and reduction extent of the catalyst. Without the addition of H_2O, the catalyst is reduced more and the yield of total oxidation products is increasing. There is clearly a particular reduction extent which gives optimal selectivity. From the quantitative results in Table 1 it can be seen that no remarkable differences in the composition between the V_2O_5/SnO_2 catalysts (1/1.5) used with or without steam addition are detected.

Adsorption of Pyridine Derivatives on Catalyst V_2O_5/SnO_2 = 1/1.5

The N_{1s} ESCA spectra from nicotinic

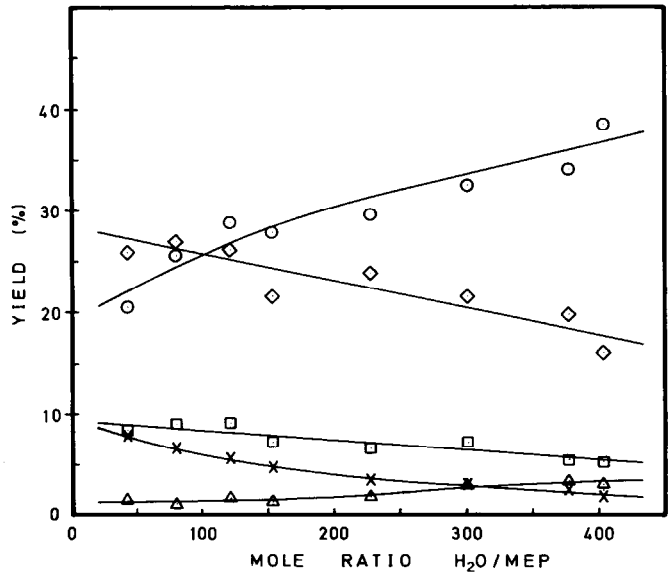

FIG. 9. The mole percentage for the conversion to some of the main products calculated per mole of incoming MEP, as a function of the mole ratio H_2O/MEP. The average of the mole ratio O_2/MEP was 75 and the temperature was 400°C. Catalyst V_2O_5/SnO_2 = 1/1.5 was used. (○) Niacin, (△) 2-methyl-5-vinylpyridine, (◇) carbon dioxide, (□) carbon monoxide, (X) Hydrogen cyanide.

acid, isonicotinic acid, picolinic acid, pyridine-2,5-dicarboxylic acid, nicotinic acid N-oxide, and isonicotinic acid N-oxide are shown in Fig. 10 and values are given in Table 3. The pyridine carboxylic acids have an N_{1s} signal at about 399.0–399.7 eV, and the N-oxides, with a more positive nitrogen atom, have an N_{1s} binding energy of about 402 eV. The picolinic acid also has a component at 400.8 eV (ratio 2 : 3). The signal at 400.8 eV is considered to be due to an intramolecularly hydrogen-bonded nitrogen atom. This is in conformity with a shift of ≃2eV upon protonation of pyridine obtained from atom charges and correlation diagram for aromatic nitrogen compounds given by Nordberg *et al.* (*35*). This is also supported by literature data; for example, a shift of ≃2eV in the N_{1s} signal between pyridine adsorbed on acid and hydroxylated oxides (*36, 37*) and between the two N-species in porphyrins (*38*). 2-Pyridine carboxylic acid is relatively easily decarboxylated (*34*) compared with 3- and 4-pyridine carboxylic acid, which may be due to the intramolecularly hydrogen-bonded form.

It can be observed in the N_{1s} core line from the pyridine derivatives that substitution in the β-position yields larger half-widths than substitution in the α- or γ-positions. This is thought to be due to larger charge delocalization with the substitution in the latter positions, since substituents in the β-position do not participate in the resonance structures.

The results from the adsorption of pyridine, 3-picoline, MEP, and pyridinecarbaldehyde on the catalyst in vacuum are shown in Table 3 and Fig. 10. See also data for the catalyst used for 150 min. It can be seen that the N_{1s} BE is approximately 399 eV. These molecules are thus adsorbed on the catalyst V_2O_5/SnO_2 (1/1.5) without any significant charge transfer from the N atom. At low temperature, where water was also condensed on the catalyst, one component at 401 eV was observed. This is thought to be due to protonation of the N atoms. It is thus thought that the pyridine derivatives

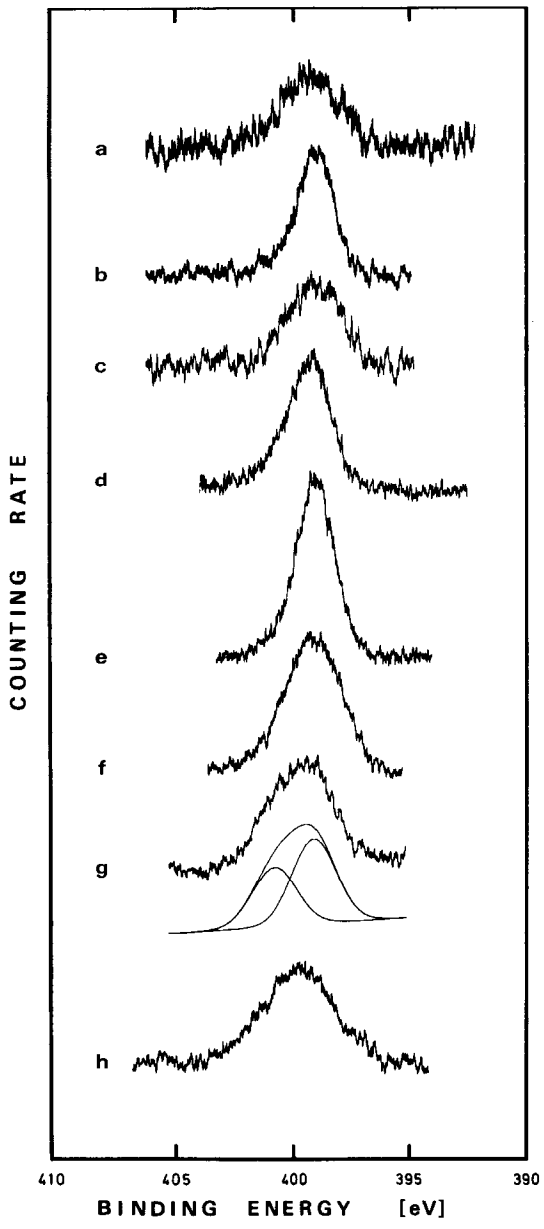

FIG. 10. N_{1s} electron spectra of some pyridine derivatives adsorbed on the catalyst V_2O_5/SnO_2 = 1/1.5 at various temperatures under vacuum. (a) V_2O_5/SnO_2 = 1/1.5 used for 150 min in the catalytic oxidation of 2-picoline, (b) V_2O_5/SnO_2 = 1/1.5 + 3-picoline, 250°C, (c) V_2O_5/SnO_2 = 1/1.5 + MEP, 250°C, (d) V_2O_5/SnO_2 = 1/1.5 + 3-pyridinecarbaldehyde, 25°C, (e) nicotinic acid, (f) isonicotinic acid, (g) picolinic acid, (h) isocinchomeronic acid.

are adsorbed on the catalyst without any involvement of the N atom. Furthermore, it has been suggested (*39*) from ir data that 2-picoline is adsorbed via the methyl group.

Since it is known that pyridine H-bonded to alumina surfaces readily desorbs during pumping at room temperature (*40*), it is possible that under the operating conditions of this catalyst there are H-bonded species, but these are not present under the conditions of the ESCA study.

If then pyridine, 3-picoline, and MEP are not adsorbed via the N atom, but are held flat, the adsorbed amounts should fall in the sequence Py > 3-picoline > MEP, since 3-picoline and MEP have bulky substituents which would render planar adsorption difficult. However, as seen in Table 3, MEP is adsorbed about 20 times greater than pyridine, and 3-picoline and pyridinecarbaldehyde about 40 times greater. This suggests that adsorption proceeds through an alkyl carbon. This type of adsorption ought to be with H-detachment and onto an O atom. The adsorbed species thereafter may desorb as an intermediate. The increase in C/Σ and O_{ad}/Σ with the reaction time may very well correspond to an increased amount of an adsorbed intermediate.

The fact that 3-picoline is adsorbed to a greater extent than MEP should have some effect on the relative activity. However, from a comparison between Figs. 7a and b where the mole ratio O_2/alkylpyridine is changed for the same catalyst, it is clear that the oxidation of MEP is more vigorous than the oxidation of 3-picoline. These results may indicate that the rate-limiting step is not the adsorption of the alkylpyridine. However, various other factors exist. An increased number of alkyl groups will increase the tendency for reaction via the alkyl groups. Furthermore, it is thought that MEP has a higher reducing capability toward V_2O_5 than 3-picoline due to the larger number of carbon atoms in the molecule. Thus there ought to be a difference in the exact state of the catalyst in the two cases. This is supported by the observation

TABLE 3

N_{1s}, O_{1s}, and C_{1s} Binding Energies (eV) and Atom Ratios N/V and O/N for Some Pyridinecarboxylic Acids, Used Catalyst, and Some Pyridine Derivatives Adsorbed on V_2O_5/SnO_2 (1/1.5)

	N_{1s}	O_{1s}	C_{1s}	N/V	O/N	Ref.
V_2O_5/SnO_2 with adsorbed:						
MEP, 250°C	399			1		
3-Picoline, 400°C	399			2.1		
Pyridinecarbaldehyde, 350°C	399.3	532.1		2.2	1.3	
Pyridine, 25°C	399.7			0.05		
V_2O_5/SnO_2 used for 150 min	399.3			0.40		
Nicotinic acid	399.0	531.4	285[a]		1.7	
Isonicotinic acid	399.2	531.7	285		2.5	
Picolinic acid	400.8–399.1	531.6	285		2.8	
Pyridine-2,5-dicarboxylic acid	399.7	531.7	285		3.4	
Nicotinic acid N-Oxide	402.2	531.2	285		2.8	
Isonicotinic acid N-Oxide	402.1	531.0	285		2.6	
Pyridine–H^+	$\Delta BE^b \simeq 2$					*35*
Pyridine, ad η–Al_2O_3	400.7					*36*
Pyridine, ad KOH–Al_2O_3	399.9–398.0					*36*
Pyridine, ad HCl–Al_2O_3	402–400					*36*
Pyridine, condensed	398.8		285			*36*
Pyridine, ad HY-zeolite	$\Delta BE^b = 2$					*37*
Porphyrins	$\Delta BE^c \simeq 2$					*38*

[a] The C_{1s} line was given the value of 285 eV to correct for sample charging.
[b] Shift relative to pure pyridine
[c] Shift between the two N_{1s} lines.

above that a higher concentration of the alkylpyridine in the vapor phase yields a more reduced catalyst.

ACKNOWLEDGMENT

The authors are grateful to Professor S. T. Lundin for his generous support during the course of this work.

REFERENCES

1. E.g., Bhattacharyya, S. K., Shankar, V., and Kar, A. K. *Ind. Eng. Chem. Prod. Res. Devel.* **5**, 65 (1966).
2. German Patent 1,940,320 (1972).
3. US Patent 2,845,428 (1958).
4. Simard, G. L., Steger, J. F., Arnott, R. J., and Siegel, L. A., *Ind. Eng. Chem.* 47(7), 1424 (1955).
5. Mars, P., and van Krevelen, D. W. *Chem. Eng. Sci. Suppl.* **3**, 41 (1954).
6. E.g., Brinen, J. S., *Accounts Chem. Res.* **9**, 86 (1976).
7. Swingle, R. S., and Riggs, W. M., *Crit. Rev. Anal. Chem.* **10**, 267 (1975).
8. Colpaert, M. N., *Z. Phys. Chem.* **84**, 150 (1973).
9. Andersson, A., and Lundin, S.-T. *J. Catal.* **58**, 383 (1979).
10. Schön, G., *J. Electron Spectrosc. Relat. Phenom.* **1**, 377 (1972/1973).
11. Johansson, G., Hedman, J., Berndtsson, A., Klasson, M., and Nilsson, B., *J. Electron Spectrosc. Relat. Phenom.* **2**, 295 (1973).
12. Järås, S. *Chromatographia* **9**, 468 (1976).
13. E.g., Fadley, C. S., *J. Electron Spectrosc. Relat. Phenom.* **5**, 895 (1974).
14. Carter, W. J., Schweitzer, G. K., and Carlsson, T. A.; *J. Electron Spectrosc. Relat. Phenom.* **5**, 827 (1974).
15. Fadley, C. S., Baird, R. J., Siekhaus, W., Novakov, T., and Bergström, S. Å. L., *J. Electron Spectrosc. Relat. Phenom.* **4**, 93 (1974); Ebel, H., and Ebel, M. F., *X Ray Spectrom.* **2**, 19 (1973).
16. E.g., Janghorbani, M., Vulli, M., and Starke, K., *Anal. Chem.* 47(13), 2200 (1975).
17. E.g., Berthou, H., and Jørgensen, C. K., *Anal. Chem.* 47(3), 482 (1975).
18. E.g., Swingle, R. S., *Anal. Chem.* 47(1), 21 (1975).
19. Okamoto, Y., Hashimoto, T., Imanaka, T., and Teranishi, S., *Chem. Lett.*, 1035 (1978).
20. E.g., Robert, T., Bartel, M., and Offergeld, G., *Surface Sci.* **33**, 123 (1972).

21. E.g., Nefedov, V. I., Gati, D., Dzhurinskii, B. F., Sergushin, N. P., and Salyn, Y. V., *Russ. J. Inorg. Chem.* **20**(9), 1279 (1975).
22. Larsson, R., Folkesson, B., and Schön, G., *Chem. Scr.* **3**(2), 88 (1973).
23. Blauuw, C., Leenhouts, F., Van der Woude, F., and Sawatsky, G. A., *J. Phys. C.* **8**, 459 (1975).
24. Hamrin, K., Nordling, C., Kihlborg, L., *Ann. Acad. Regiae Sci. Ups.* **14**, 70 (1970).
25. Bird, R. J., *Met. Sci. J.* **7**, 109 (1973).
26. Grutsch, P. A., Zeller, M. V., and Fehlner, T. P., *Inorg. Chem.* **12**(6), 1431 (1973).
27. Ansell, R. O., Dickinson, T., Povey, A. F., and Sherwood, P. M. A., *J. Electron Spectrosc. Relat. Phenom.* **11**, 301 (1977).
28. Itoh, M., Hattori, H., and Tanabe, K., *J. Catal.* **43**, 192 (1976).
29. Praliaud, H., and Mathieu, M.-V., *J. Chim. Phys.* **73**(5), 509 (1976).
30. Shulga, Y. M., Ivleva, I. N., Shimansk, M. V., Margolis, L. Y., and Borodko, Y. G., *Zh. Fiz. Khim.* **49**(11), 2976 (1975).
31. Valdelièvre, M., Dechy, G., and Leroy, J.-M., *C. R. Acad. Sci. Ser. C* **276**, 1179 (1973).
32. Gillis, E., and Boesman, E., *Phys. Status Solidi.* **14**, 337 (1966).
33. E.g., Norton, P. R., *Surface Sci.* **47**, 98 (1975).
34. Järås, S., and Lundin, S.-T., *J. Appl. Chem. Biotechnol.* **27**, 499 (1977).
35. Nordberg, R., Albridge, R. G., Bergmark, T., Ericson, U., Hedman, J., Nordling, C., Siegbahn, K., and Lindberg, B. J., *Ark. Kemi* **28**(19), 257 (1967).
36. Gati, G., Nefedov, V. I., and Szalin, J. W., *Mag. Kem. Foly.* **80**(10–11), 514 (1974).
37. Defossé, C., and Canesson, P., *J. Chem. Soc. Faraday I* **72**, 2565 (1976).
38. Lavallee, D. K., Brace, J., and Winograd, N., *Inorg. Chem.* **18**(7), 1776 (1979).
39. Leitis, L. Y., Shimanskaya, M. V., and Slavinskaya, V. A., *Chem. Heterocycl. Comp.* **4**(2), 772 (1968).
40. Knözinger, H., *Advan. Catal.* **25**, 184 (1976).